Available online at www.sciencedirect.com
ScienceDirect
Sensors and Actuators A 132 (2006) 689–700
SENSORS AND ACTUATORS A PHYSICAL
www.elsevier.com/locate/sna

Pneumatically actuated micromachined synthetic jet modulators

David J. Coe [a,*], Mark G. Allen [b], Christopher S. Rinehart [c], Ari Glezer [c]

[a] *Electrical and Computer Engineering Department, University of Alabama in Huntsville, Huntsville, AL 35899, United States*
[b] *School of Electrical and Computer Engineering, Georgia Institute of Technology, Atlanta, GA 30332, United States*
[c] *School of Mechanical Engineering, Georgia Institute of Technology, Atlanta, GA 30332, United States*

Received 11 February 2005; received in revised form 30 January 2006; accepted 4 February 2006
Available online 3 April 2006

Abstract

Results presented in the synthetic jet literature have focused on the demonstration of and application of one or more *single-orifice* synthetic jet actuators in jet vectoring and other aerodynamic applications. For these applications, amplitude and phase modulation techniques are often used in conjunction with the oscillatory nature of the synthetic jet flow to achieve the desired results. In this work the authors present a *multi-orifice synthetic jet* actuator and investigate the feasibility of using integrated microvalves for dynamic orifice output modulation. A multi-orifice synthetic jet consists of a micromachined orifice array with integrated microvalves for flow modulation and a shared membrane actuator for synthetic jet generation.

Individual orifice output modulation using microvalves could be used to compensate for manufacturing-induced or spatial variations in orifice output in a multi-orifice synthetic jet. Moreover, dynamic orifice output modulation could also be used to alter locally the zero net-mass-flux nature of the synthetic jet flow, producing localized flow regions over the multi-orifice synthetic jet in which the net-mass-flux is *positive* or *negative* instead of zero as in the case of traditional single-orifice synthetic jets. For instance, if a single oscillatory actuator is used to generate in parallel synthetic jet flow from an array of orifices, the microjet modulator associated with a particular orifice could be sequenced to open only during the intake (or exhaust) stroke of the actuator, creating a localized low (or high) pressure region at the given orifice. The use of dynamic modulation to create these localized regions with non-zero net mass flux could be harnessed to improve the efficiency synthetic jets in jet vectoring, flow control, or other applications.

This paper discusses the fabrication and characterization of pneumatically actuated, micromachined synthetic jet modulator arrays and demonstrates the use of these synthetic jet modulators for dynamic modulation of multi-orifice synthetic jet flows. The multi-orifice synthetic jet presented here utilizes a traditionally machined synthetic jet actuator for generation of synthetic jet flows (5–20 m/s) and an array of individually addressable micromachined synthetic jet modulators for manipulation of the resulting synthetic jet flows. Included are qualitative and quantitative experimental results that demonstrate static on-off modulation and dynamic flow modulation at the jet generation frequency. Continuous variation of the output of individual jets from suction-only operation to exhaust-only operation was achieved by changing the phase of the modulation signal relative to the jet generation signal. Also presented is phase formulation of the modulated synthetic jet flow, which compares favorably with measurements of the exit pressure of the modulated synthetic jet flow. A sample application of the pneumatic microjet modulator array, a lateral air pump, is also presented to demonstrate the use of dynamic synthetic jet modulation to create localized regions with non-zero net mass flux.

Keywords: Synthetic jet actuator; Micromachined synthetic jet actuator; Microjet; Microjet modulator; Dynamic synthetic jet modulation

1. Introduction

The utility of zero-net-mass-flux synthetic jet actuators has been demonstrated in a variety of applications including jet vectoring, modification of aerodynamic characteristics, thermal management of integrated circuits, and micropropulsion [1–10]. Microfabrication of synthetic jet actuators (microjets) and actuators for modulation of synthetic jet flows (microjet modulators) offers several important advantages over conventional fabrication techniques. Micromachining facilitates the integration of large numbers of synthetic jets into addressable arrays, which would allow these microactuators to be either coordinated to achieve macro-scale effects or individually addressed and phased as needed. Micromachined synthetic jets may also

* Corresponding author. Tel.: +1 2568243583; fax: +1 2568246803.
E-mail address: coe@ece.uah.edu (D.J. Coe).

0924-4247/$ – see front matter © 2006 Elsevier B.V. All rights reserved.
doi:10.1016/j.sna.2006.02.032

be integrated with microsensors and control electronics for closed-loop control over jet flow parameters. The authors have previously presented the fabrication and characterization of micromachined synthetic jet actuators [11] and demonstrated static operation of electrostatically-actuated microjet modulator arrays [12].

Unlike previously published results [1–11] that utilized drive signal amplitude and phase modulation with respect to *single-orifice* synthetic jets, the work presented here investigates the feasibility of using microvalves to modulate individual orifice output in a *multi-orifice* synthetic jet. A *multi-orifice* synthetic jet uses a single shared membrane or piston to generate synthetic jet flow through an array of orifices simultaneously. As presented here, the multi-orifice synthetic jet configuration combines a separately machined, large displacement actuator for synthetic jet generation and a micromachined orifice array with integrated microvalves for modulation of individual orifice output. Such a configuration may simplify manufacturing. Moreover, the integration of microvalve modulators should facilitate tuning of the synthetic jet output to match the needs of the application.

Dynamic orifice-by-orifice output modulation could be used to compensate for spatial or manufacturing-induced orifice output variations in a multi-orifice synthetic jet. The oscillatory nature of the synthetic jet also suggests that dynamic microvalve modulation of the synthetic jet flow can be used to produce localized flow regions in which the net-mass-flux is non-zero. For instance, if a single oscillatory actuator is used to generate synthetic jet flow from an array of orifices, the modulator associated with a particular orifice could be sequenced to open only during the intake (or exhaust) stroke of the actuator, creating a localized low (or high) pressure region at the given orifice. The use of dynamic modulation to create these localized regions with non-zero net mass flux (flow sources and sinks) could improve synthetic jet performance in jet vectoring, micro mixing, or other applications.

In this paper the operation of pneumatically actuated micromachined synthetic jet modulators will be discussed along with experimental results from fabricated microjet modulator arrays. The hybrid design presented here utilizes a traditionally machined synthetic jet actuator for generation of higher velocity jet flows (5–20 m/s) when compared to electrostatic actuation (less than 1 m/s) [9], and an array of individually-addressable micromachined synthetic jet modulators for manipulation of the resulting synthetic jet flows. A sample application of the pneumatic microjet modulator array, a lateral air pump, is also presented to demonstrate the use of dynamic synthetic jet modulation to create localized regions with non-zero net mass flux.

2. Synthetic jet operation and modulation

A synthetic jet actuator consists of a fixed actuator cavity bound on one side by a flexible membrane and on the other by an orifice (Fig. 1). When the membrane is vibrated rapidly, air is repeatedly drawn into the cavity through the orifice (Fig. 1(a)) and then ejected out of the cavity through the same orifice (Fig. 1(b)) [2,3]. As the outgoing flow passes the sharp edges of the orifice, the flow separates forming a vortex ring, which propagates normally away from the orifice plate. Vibration of the membrane results in a train of vortices, which are formed at the excitation frequency. As in larger-scale geometries [13], the nominally round, turbulent jet is synthesized by the interaction of these vortices downstream from the orifice.

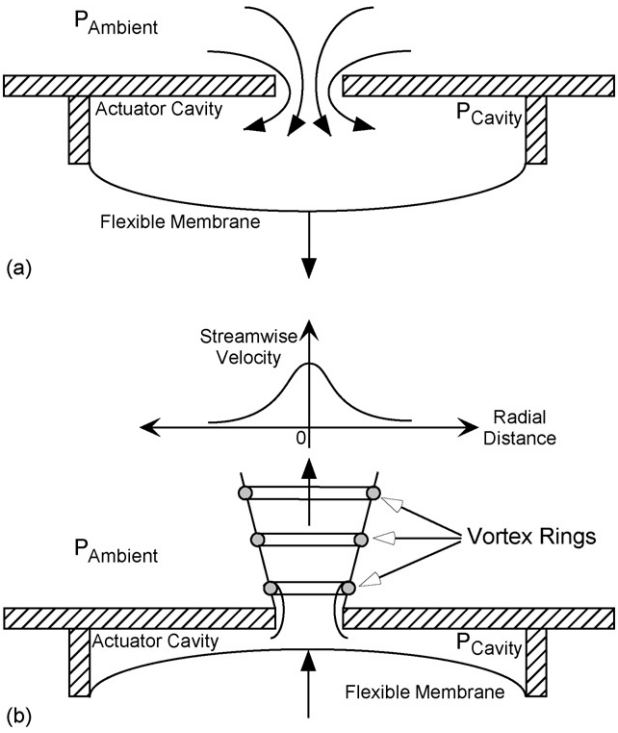

Fig. 1. Cross-section of a typical synthetic jet actuator showing both the (a) suction and (b) exhaust stages of operation.

An important feature of synthetic jets is that they are *zero-net-mass-flux* in nature; i.e., they are synthesized from ambient fluid, which is entrained and then ejected from the device. As such, the jets allow momentum transfer into the surrounding fluid without net mass injection into the overall system, thus eliminating the need for input piping and complex fluidic packaging. These attributes of synthetic jets make them ideally suited for fabrication using micromachining techniques that enable low cost fabrication, realization of large arrays, and the potential for integration of control electronics.

A synthetic jet modulator is used to vary with time the oscillatory flow in and out of a synthetic jet orifice in a microjet orifice array. As defined here, a synthetic jet modulator will provide addressability, allowing the output of an arbitrary orifice in the orifice array to be switched on and switched off. Additionally, a synthetic jet modulator will provide orifice output regulation, which is the ability to vary the output of an orifice from its minimum value to its maximum value. If the modulator can provide both addressability and output regulation at the synthetic jet excitation frequency, a synthetic jet modulator creates unique functionality that can-

not be obtained from an unmodulated synthetic jet. By varying the phasing between the synthetic jet generation signal and the jet modulation signal, a synthetic jet modulator can create flow sources (with positive, outgoing jet velocities) and flow sinks (with negative, inflowing jet velocities) within the orifice array.

3. Pneumatic actuated synthetic jet modulator operation

The pneumatic synthetic jet modulator array uses flexible latex or silicone rubber membranes to control passage of the synthetic jet flow through micromachined channels in the silicon substrate. Fig. 2 illustrates the pneumatically-actuated synthetic jet modulator concept. The externally generated synthetic jet flow passes through a central 1 mm square flow channel through the center of the silicon modulator chip. The plenum formed by the spacer layer allows the airflow to spread to reach the orifices of the orifice array chip positioned above. A flexible rubber layer is adhered to the top surface of the actuator chip. Individually controllable membranes are formed where circular holes have been etched through the actuator chip. These membranes act as normally open pneumatic microvalves as shown in Fig. 2(a). When pressure is applied to a membrane from outside the device, the released membrane deflects towards the orifice hole positioned above it as shown in Fig. 2(b) where the deflected membrane restricts synthetic jet flow through its orifice. When fully deflected, the membrane molds itself to the edge of the orifice hole creating an airtight seal. Release of the applied actuation pressure causes the stretched membrane to return to its original open position.

4. Fabrication of the pneumatic microjet modulator array

The similarity in the structure of the modulator array components, as diagrammed in Fig. 2, allows all three components of the microjet modulator array to be fabricated in parallel from the same silicon wafer using the fabrication process outlined in Fig. 3. Starting with a thermally oxidized 2” diameter silicon wafer, a single photolithography step is used to transfer the desired component geometries from the mask to a layer of thick-film photoresist (Shipley SJR-5240) spin coated onto the silicon substrate. After developing and hard baking the exposed resist, a buffered hydrofluoric acid solution (BOE) is used to complete the transfer of the mask pattern into the silicon dioxide layer. Without removing the photoresist layer, a very thin layer of heat sink grease is applied to the unpolished side of the wafer, and the wafer is placed onto a previously prepared handle wafer for the silicon etch. Handle wafer preparation consists of a single coating of thick-film photoresist (Shipley SJR-5740) that has been thoroughly baked to remove all solvents. With the sample mounted on the handle wafer, the airflow passages can then be etched through the silicon sample using the Bosch deep silicon trench etching process in a Plasma-Therm Inductively Coupled Plasma etcher (ICP). Using this process, typical etch times of 3 h were required to etch completely through the 300 μm thick 2” silicon wafers. After completion of the silicon etch process, the modulator array components were detached from the handle wafer by a four-step solvent cleaning procedure (trichloroethylene [TCE], acetone, methanol, and deionized water). Note that this procedure also removes any remaining photoresist. Once released, the silicon components are ready for assembly.

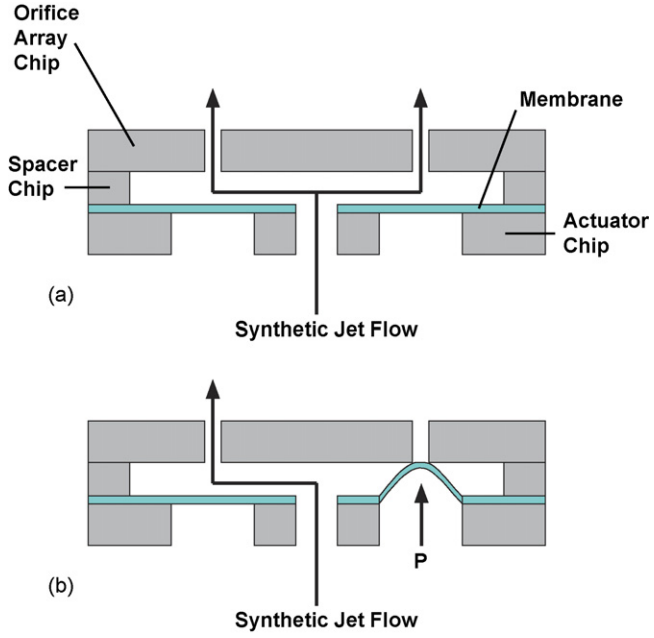

Fig. 2. Cross-section of pneumatically actuated synthetic jet modulator array showing both the deflected (spherical) and undeflected (flat) polymer membranes. (a) Shows the pneumatic modulators in their normally open default state. (b) Shows closure of the right modulator for applied pressure *P*.

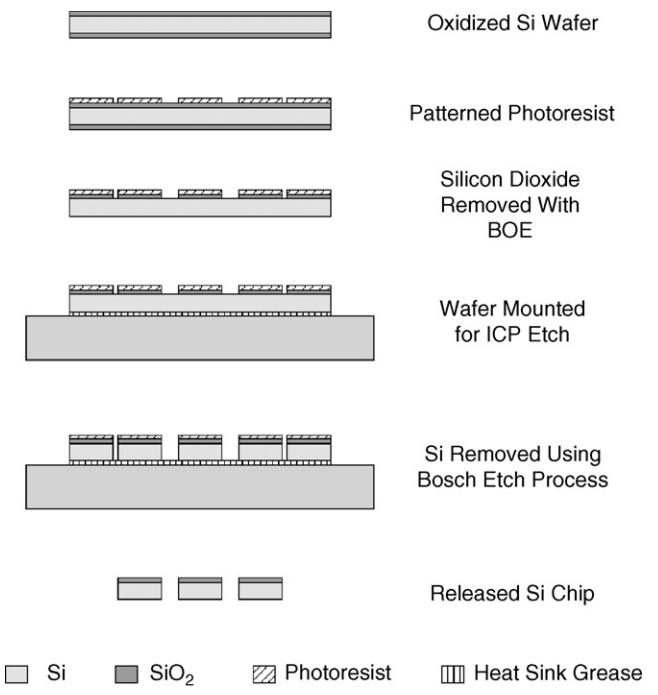

Fig. 3. Steps used for microfabrication of pneumatic microjet modulator array components.

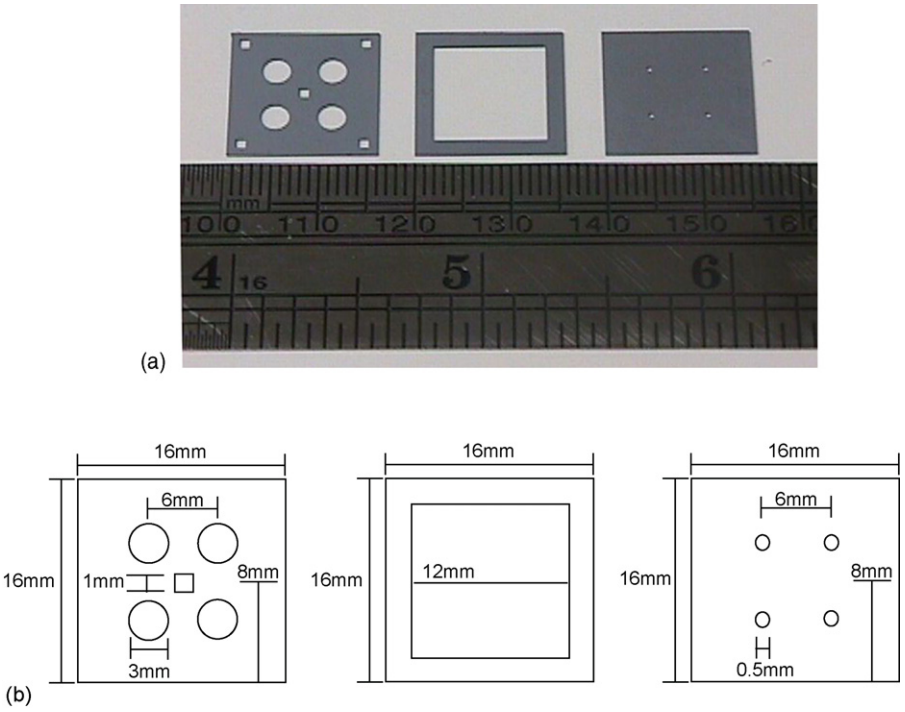

Fig. 4. Actuator, spacer, and orifice chips prior to assembly. (a) Photograph of the actuator, spacer, and orifice chips prior to pneumatic modulator assembly. (b) Diagram of the three chips including feature dimensions.

Photographs of the three silicon chips used to assemble a pneumatic synthetic jet modulator array are shown in Fig. 4(a) along with a ruler for scale. Each chip measures 16 mm × 16 mm on a side and is 300 μm thick (see Fig. 4(b)). In the center of the modulator chip, the leftmost chip pictured, the 1 mm × 1 mm synthetic jet flow channel is clearly visible along with the 2 mm × 2 mm square alignment holes etched in each corner of the chip and the four 3 mm diameter microvalve modulator holes, spaced 6 mm center to center. In the center of the photograph, the spacer chip is used to form the plenum located between the actuator and orifice chips. Finally, the 2 × 2 array of 500 μm orifices, also spaced 6 mm center to center, are clearly visible in the orifice chip, pictured on the far right side of the photograph.

The photographs appearing in Fig. 5 show the micromachined synthetic jet modulator array during various stages of assembly. The proof-of-concept devices presented here were manually assembled layer-by-layer using a mechanical alignment jig to align the three chips during the bonding process. Fig. 5(a) shows the actuator chip with the adhesively bonded 150 μm thick silicone rubber membrane mounted onto an aluminum sample plate for testing. A mechanical punch was used to define the hole through the center of the rubber membrane prior to bonding. Epoxy bonding of the unstretched rubber membrane to the actuator chip occurred at room temperature in an effort to minimize device-to-device membrane tension variations. Fig. 5(b) shows the mounted sample after bonding of the spacer chip, and Fig. 5(c) shows the modulator array after addition of the orifice array chip. Close inspection of Fig. 5(a) and (b) indicates variation in movable membrane area due to adhesive flow. Finally, the photograph in Fig. 5(d) shows the fully assembled pneumatic synthetic jet modulator array ready for testing.

For this feasibility study, the device dimensions have not been selected to optimize either synthetic jet performance or microvalve modulator performance. Dimensions have been selected primarily to address fabrication constraints, including manual alignment and bonding of chip layers, and characterization constraints, including the use of pressure tube measurement equipment.

5. Test setup

As indicated above, each fully assembled device is attached to its own aluminum sample plate to facilitate uniform testing from one device to the next. Fig. 5(d) shows a typical device bonded to a sample plate. The four holes, one in each corner of the sample plate, allow the entire assembly to be bolted to the aluminum test fixture that contains the audio speaker and the pneumatic actuation ports. Once testing on a given device is complete, it can be easily removed from the test fixture and replaced with another device. The use of a common shared test fixture is intended to reduce performance variations that may result if separate test assemblies are used for characterization of each device.

A test fixture was needed that could both direct flow from the external synthetic jet source into the plenum area of the modulator array chip and direct pneumatic actuation pressure to the individual membrane modulator microvalves. A cross-section of the machined aluminum test fixture is presented in

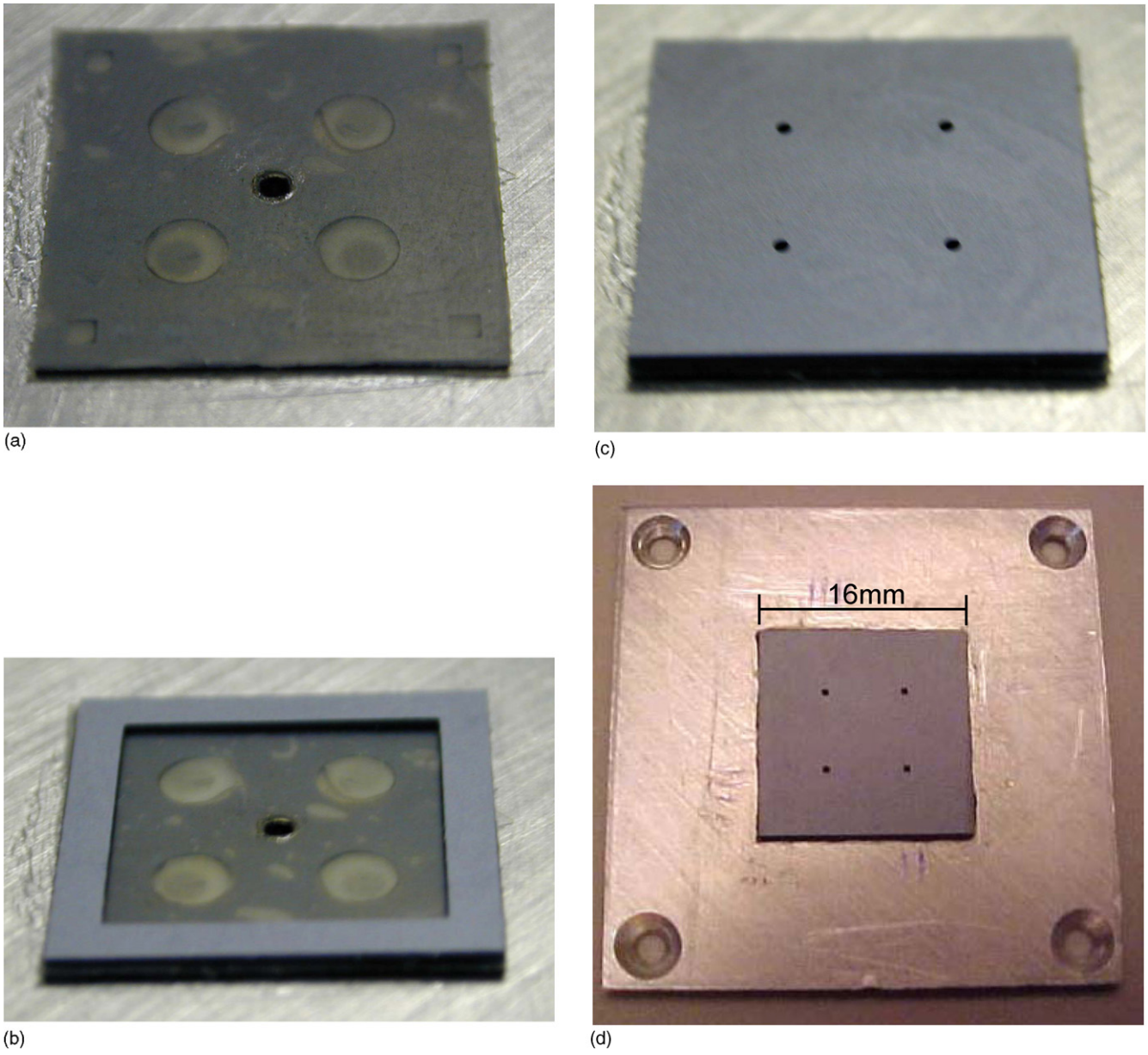

Fig. 5. Photographs of pneumatic microjet modulator array during assembly. (a) Mounted actuator chip with attached membrane. (b) After addition of spacer chip. (c) After addition of orifice array chip. (d) Fully assembled pneumatic microjet modulator array mounted for testing.

Fig. 6. Note that a centrally located channel is used to direct the oscillatory flow generated by an external audio speaker into the plenum of the synthetic jet modulator array, and that machined flow channels are used to direct the pneumatic control pressures from the external pneumatic actuation ports of the test fixture to the individual synthetic jet modulators. A rubber gasket, located between the sample plate and test fixture, was used to prevent crosstalk between the flow channels.

A pneumatic modulation control system was created to convert the electrical control signals into pneumatic control signals by using an array of three-way solenoid valves connected to a pressure distribution manifold as shown in Fig. 7. By default, a three-way solenoid valve would connect a pneumatic actuation port to the common pressure relief vent of the manifold, which was held at atmospheric pressure so that the microvalve modulator membranes would remain in their normally open position. To close a modulator, the three-way solenoid valve would connect that pneumatic actuation port to the common regulated pressure inlet of the manifold, applying sufficient pressure to fully deflect the modulator membrane to its closed position. Opening of a closed modulator was achieved by returning the three-way solenoid valve to its default position, which allowed the previously applied pressure to escape through the common pressure relief port of the manifold.

The particle image velocimetry system (PIV) described in Fig. 8 was used for qualitative characterization of the modulated synthetic jet flows. During PIV testing the aluminum test fixture, with mounted modulator array sample, are placed within

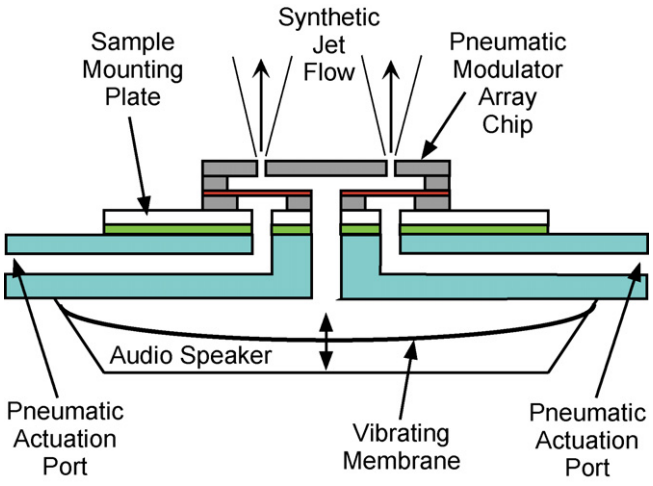

Fig. 6. Cross-section of pneumatic microjet modulator array test fixture.

a clear glass enclosure. Using a system of lenses, the beam from a two head Nd:YAG laser system is shaped into a thin sheet and used to illuminate smoke particles in the flow field emanating from the modulated microjets. Under computer control, a high speed, high-resolution video camera was used to photograph movement of the smoke particles. Each measurement requires acquisition of a pair of images, one at time t and one at time $t + \Delta t$, where the operator using the computer software set the time interval Δt. Given the physical distance per pixel and the time interval Δt, image-processing software could then compute the corresponding velocity vector for each particle in the image, producing a two-dimensional velocity vector map. Multiple vector maps would then be averaged to determine the average velocity vectors.

The miniature pressure tube measurement apparatus shown schematically in Fig. 9 was used for quantitative characterization

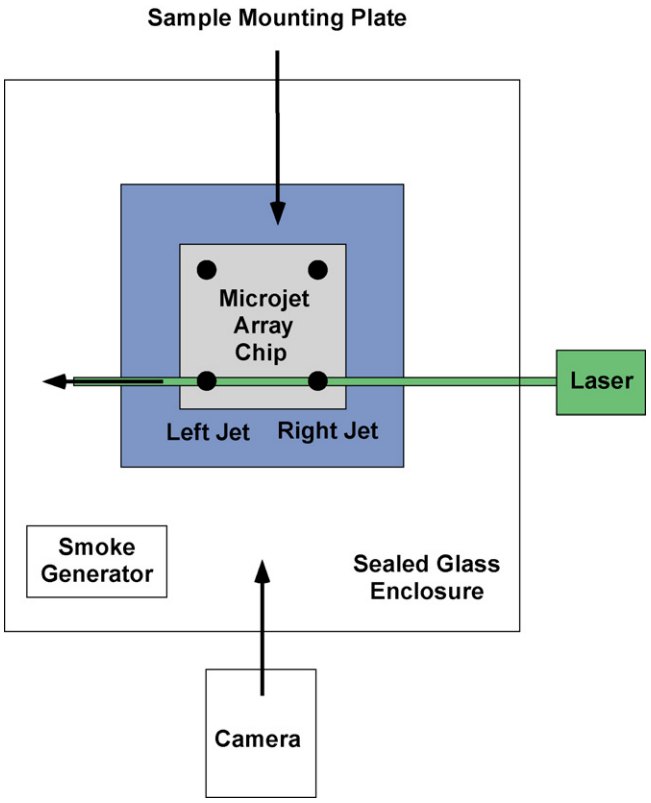

Fig. 8. Conceptual diagram of particle image velocimetry (PIV) measurement setup.

of the microjet modulator array. The aluminum test fixture with the mounted modulator array sample was positioned beneath the miniature pressure tube (212 μm inner diameter, 340 μm outer diameter, 25 mm length) such that the synthetic jet flow from an orifice was directed into the pressure tube. The micromachined differential pressure sensor was used to measure pressure

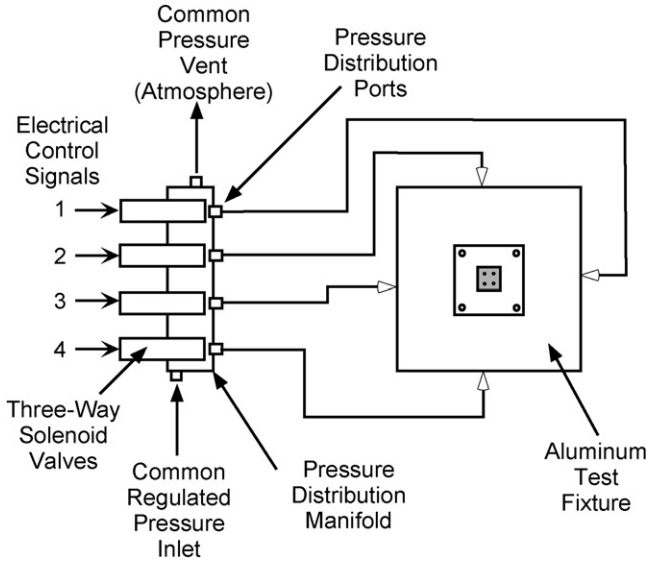

Fig. 7. Schematic of pneumatic microjet modulation control system for conversion of electrical control signals into pneumatic control signals.

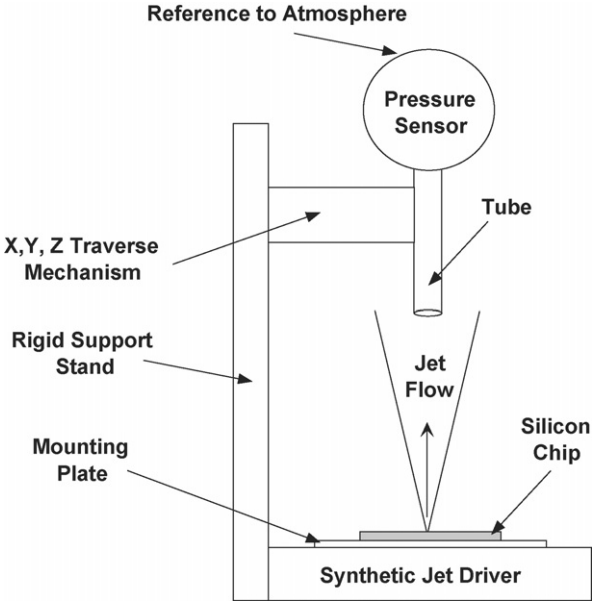

Fig. 9. Pressure tube test setup.

changes, relative to its reference port, resulting from the synthetic jet flows.

6. Testing of the microjet modulator array

Qualitative and quantitative tests were performed to demonstrate that the pneumatically actuated synthetic jet modulator array was fully functional. First, the DC operation of the modulators was observed using the PIV system. The transient switching characteristics of the modulators were assessed using pressure measurements. Finally, pressure measurements were also used to monitor flow changes due to phase variations between the modulation signal and the synthetic jet formation.

6.1. DC operation of microjet modulators

The aluminum test fixture, with a mounted microjet modulator array sample, was placed into the PIV system and aligned such that the flow from an adjacent pair of orifices could be observed as shown in Fig. 8. For this experiment, flow from the other orifice pair, located out of the viewable area, was temporarily disabled so that leaking testing could be performed on the orifice pair under test. PIV system length scales were calibrated using measured spacing of chip features, and time scale calibration of the instrument was factory set. A function generator was used to generate a 20 Hz sinusoidal waveform that was delivered to the audio speaker for synthetic jet generation via a standard audio amplifier.

For this feasibility study, an 89 mm diameter speaker was mounted to the aluminum test fixture for synthetic jet generation. Although optimized for operation at higher frequencies, the speaker when excited at 20 Hz produced a synthetic jet flow from the multi-orifice chip that could be measured with the available pressure transducer. Selection of a small diameter speaker also reduced the overall cost associated with the fabrication of the aluminum test fixture. The use of removable aluminum sample plates allowed the same speaker-amplifier combination to be used in the characterization of all fabricated devices, eliminating measurement variations due to the use of different speakers or amplifiers with each fabricated device. Device performance could be improved by optimizing selection of the speaker-amplifier combination to final device geometry and operating frequency.

A second function generator was used to trigger the PIV computer to record image pairs from the camera in 5° increments for the entire 360° span of the sinusoidal waveform period using a Δt of 25 μs. The resulting velocity vector maps from each increment were then averaged to produce an average velocity vector map. The pneumatic modulation control system was used to apply 34.5 kPa (5 psi) control pressure to each modulator in turn and then to both modulators simultaneously to cycle through the four permutations of two jet DC operation (On:On, On:Off, Off:On, and Off:Off). The resulting average velocity maps are shown in Fig. 10(a) and (d). Note that as designed for an applied pressure of 34.5 kPa, each modulator membrane not only deflects 300 μm, the thickness of the spacer chip, but no leaks from the orifices are observed when the jet flow is supposed to be off.

6.2. Measurement of modulator switching properties

The switching characteristics of the modulators were measured by temporarily replacing the audio speaker used for synthetic jet generation with a gas line connected to a pressure regulated nitrogen source to produce a continuous jet flow from each orifice. The miniature pressure sensor tube was then positioned using the XYZ traversing system at the center of an orifice with the tip of the pressure tube aligned with the orifice exit plane. The delivered nitrogen pressure was varied to produce an orifice exit velocity comparable to the velocities observed using the PIV system (nominally 11 m/s). A digital oscilloscope was then used to record simultaneously the step function modulation signal used to open or close the modulator and the resulting output of the differential pressure sensor. Fig. 11 shows the resulting measured pressures. Note that the closing time of the modulator is 12 ms and the opening time of the modulator is 30 ms for a total cycle time of 42 ms. The modulator is thus capable of operating at the same frequency used for synthetic jet generation, 20 Hz.

Using the same experimental setup, the pressure induced by the continuous jet, modulated at 20 Hz by the synthetic jet modulator, was measured by applying a 20 Hz, 50% duty cycle square wave input to the appropriate solenoid control valve of the pneumatic modulation control system. As seen in Fig. 12, the 50% duty cycle modulation signal does not produce 50% modulation (equal flow off and flow on times) due to the asymmetric opening and closing times of the microvalve modulator. Variation of the modulation signal duty cycle, however, results in a close approximation of 50% modulation as shown in Fig. 13 using a 40% duty cycle modulation signal.

Another interesting feature of the output signal pictured in Fig. 13 is that a periodic ringing is seen in the pressure sensor output in both the modulator-open and modulator-closed states. It is speculated that this ringing is due to the mechanical resonance of the pressure sensor element and is induced by the relatively sudden transitions between full flow and zero flow. Full flow from the orifice dampens the magnitude of the ringing somewhat, but it is still visible across the entire sensor output range, even during transitions between full flow and zero flow.

6.3. Phase modulation of synthetic jet flow

After reinstallation of the speaker for synthetic jet generation, the induced pressure was measured as the phase angle between the 20 Hz synthetic jet signal and the 20 Hz, 50% duty cycle modulation signal was varied (in this experiment the tip of the pressure tube was placed 500 μm ($x/D = 1$) downstream from the orifice exit plane). The three remaining orifices remained open during this measurement. Fig. 14 shows the measured pressure for phase angles from 0 to 360° in 10° increments for four different orifices. Note that there are two distinct operating regimes. For a range of phase angles (typically between 45 and 170°), the pressure is negative when the orifice acts as a flow sink, and for the remaining phase angles, the pressure is positive when the orifice acts as a flow source. While the exact causes of the variations in device performance are under investigation,

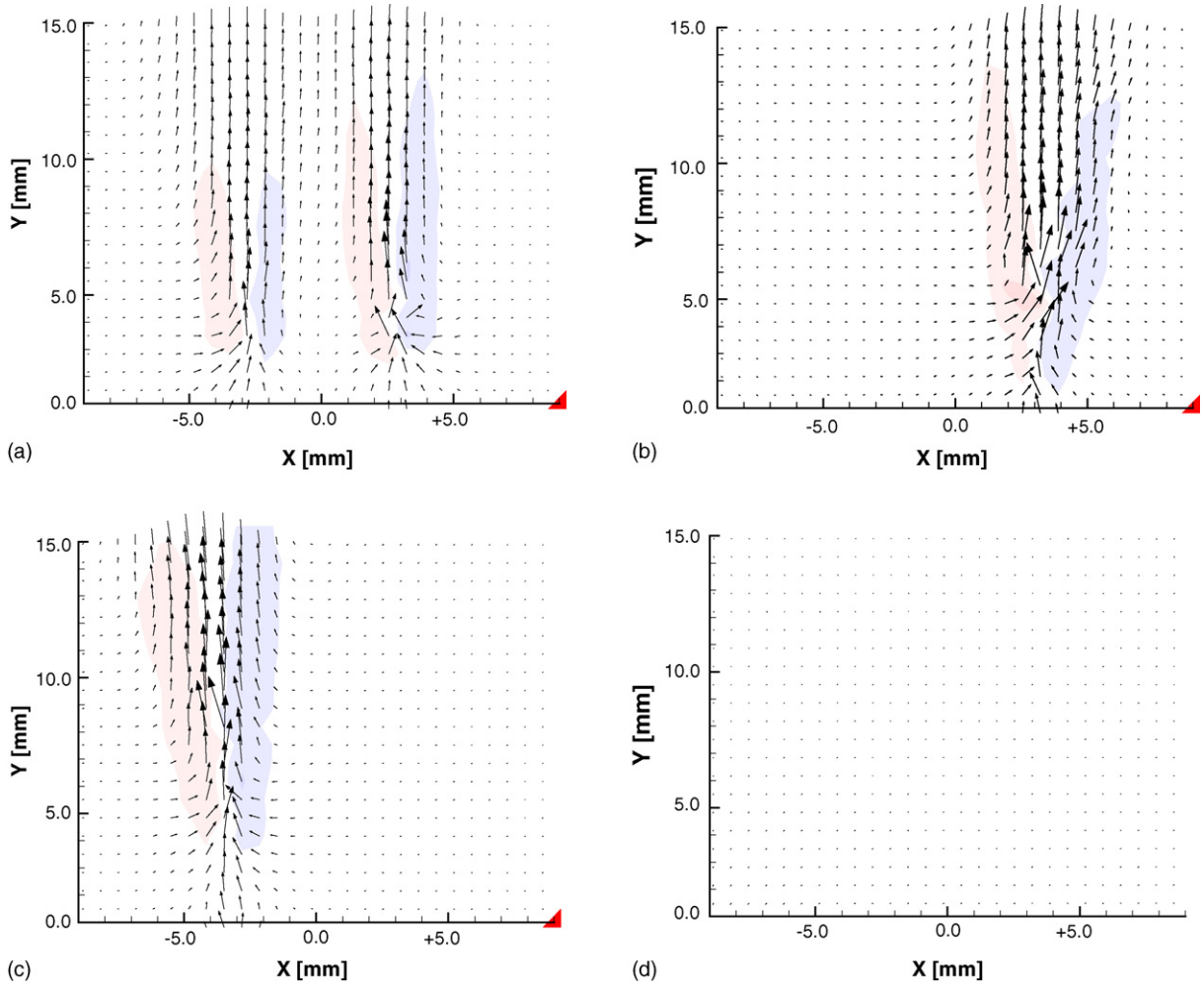

Fig. 10. PIV velocity vector plots showing the DC static operation of two pneumatic modulators. (a) Shows the two modulators in their normally open state. (b) Shows the left modulator closed with the right one open. (c) Shows the right modulator closed with the left one open. (d) Shows both modulators closed.

possible causes include propagation delay differences due to misalignment during the manual assembly process, mechanical variations in membrane operation due to adhesive flow or non-uniform membrane tension, variations in the operation of the pneumatic control system, and inconsistencies in the placement of the measurement probe.

7. Modulated synthetic jet flow formulation

The induced pressure of the modulated synthetic jet was modeled to formalize the analysis of the measured pressure. Assuming that the exit pressure of the unmodulated synthetic jet is sinusoidal with frequency f and amplitude P_0, then the exit pressure p as a function of time t may be written as in Eq. (1).

$$p(t) = P_0 \sin(2\pi f t) \tag{1}$$

To model the flow modulation, first assume that the ideal modulator operates at a frequency f with a 50% duty cycle such that the flow off and flow on times are equal. If $\tau(t)$ represents the pressure function of the modulator, the pressure transmitted by the modulator as a function of time t, then $\tau(t) = 1$ when the modulator is open, and $\tau(t) = 0$ when the modulator is closed. $\tau(t)$ may be described by Eq. (2) where $\text{sign}(x) = -1$ if $x < 0$, 0, if $x = 0$, and 1 if $x > 0$.

$$\tau(t) = \frac{\text{sign}[-\sin(2\pi f t)] + 1}{2} \tag{2}$$

Note that $\tau(t)$ is a square wave of amplitude 1 with a value of 0 for its first half period and a value of 1 for its last half period.

The exit pressure of the modulated flow $m(t)$ may thus be described by Eq. (3) where θ is the phase shift in degrees and T is the period of the waveform.

$$m(t) = p(t)\tau\left(t + \left(\frac{\theta}{360^\circ}\right)T\right) \tag{3}$$

Note that this formulation does not account for propagation time t_{prop} through the device (the time between a change in the speaker input and a measurable pressure change at an orifice) and the non-instantaneous opening time of the modulator itself t_{shift}. Modifying Eq. (3) to account for these non-idealities yields the practical model of modulated flow $m^*(t)$ as shown in Eq. (4).

$$m^*(t) = p(t + t_{\text{prop}})\tau\left(t + t_{\text{prop}} - t_{\text{shift}} + \left(\frac{\theta}{360^\circ}\right)T\right) \tag{4}$$

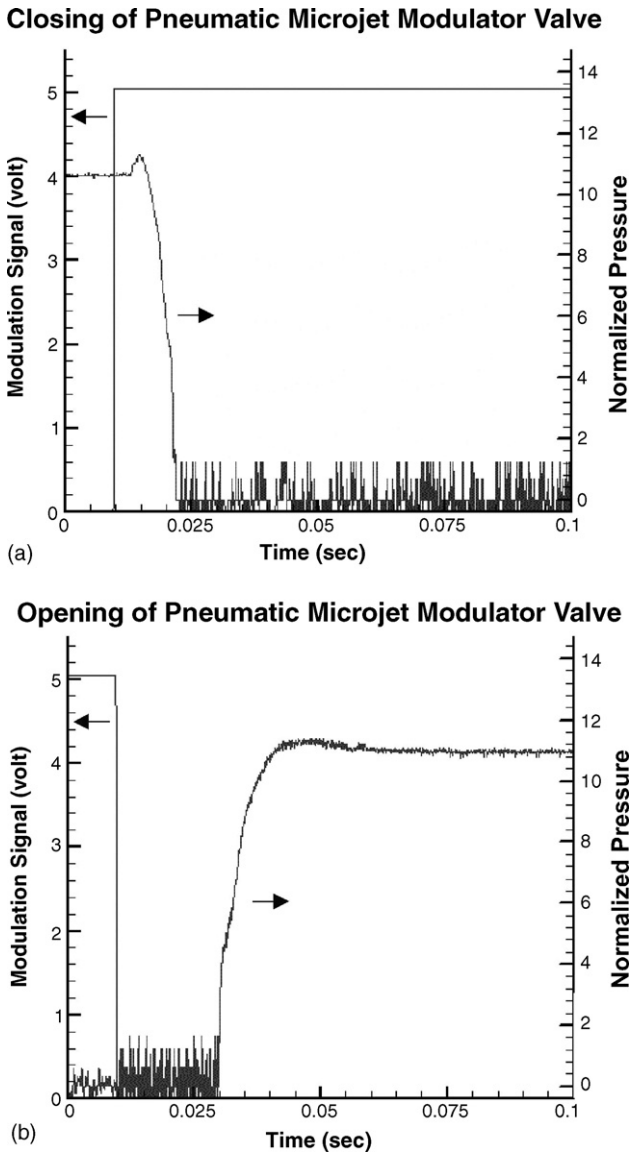

Fig. 11. Transient performance of a pneumatically actuated microvalve modulator measured using the pressure tube and continuous jet source. (a) Closing [modulation signal rising edge] and (b) opening [modulation signal falling edge].

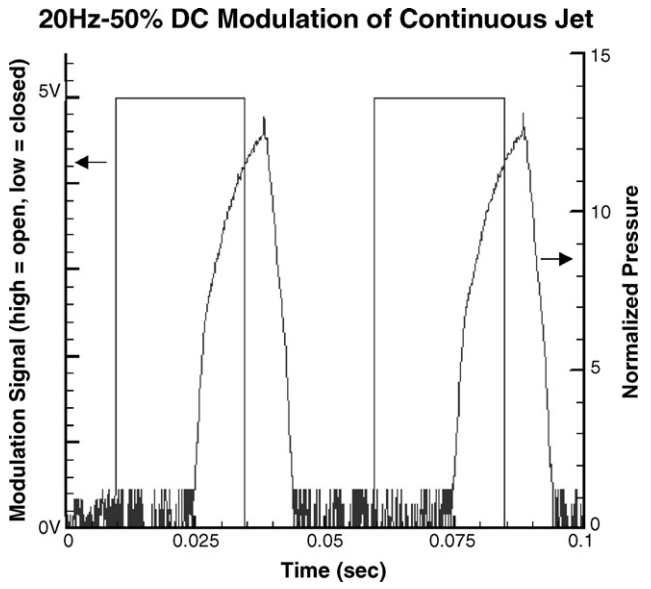

Fig. 12. Measured pressure in a continuous jet modulated using a 20 Hz, 50% duty cycle square wave modulation signal.

8. Validation of modulated flow formulation

The formulation assumes that a sinusoidal waveform is used to generate the synthetic jet, that the ideal modulator achieves 50% modulation, and that the synthetic jet generation signal and modulation signal are at the same frequency. As previously observed (Fig. 13), to achieve 50% modulation, the duty cycle of the modulation waveform must be adjusted to compensate for the asymmetric modulator opening and closing times. Since a 20 Hz sinusoidal waveform is used to generate the synthetic jet, a 20 Hz, 40% duty cycle waveform is used to modulate the resulting flow since this is the best approximation of the ideal 50% modulation. The closing time of the modulator t_{shift} was previously determined to be 12 ms from measurements made using the continuous jet source (Fig. 11). The propagation delay t_{prop} of 1.1 ms was determined by measuring the time between a step function input to the speaker and a measurable pressure change at the orifice exit. The formulation also assumes that $m^*(t)$ is the exit pressure so the end of the pressure tube is positioned at the orifice exit plane. Finally, the amplitude of the unmodulated synthetic jet exit pressure P_0 was measured and used for normalization.

The phase modulation experiments were repeated, and transient pressure was measured at the exit plane. Fig. 15 shows a comparison of the measured data and the formulation results for phase shifts of 0, 90, 180, and 270°. In all four cases, the theoretical curves derived from the formulation $m^*(t)$ are consistent with the measured values of exit pressure. For phase shifts of 0 and 180°, the switching times of the pneumatically actuated micromachined synthetic jet modulators are still visible in the measurements (near the rising and falling edges of the theoretical curves), but the selection of a 40% duty cycle modulation signal has resulted in near 50% modulation of the synthetic jet.

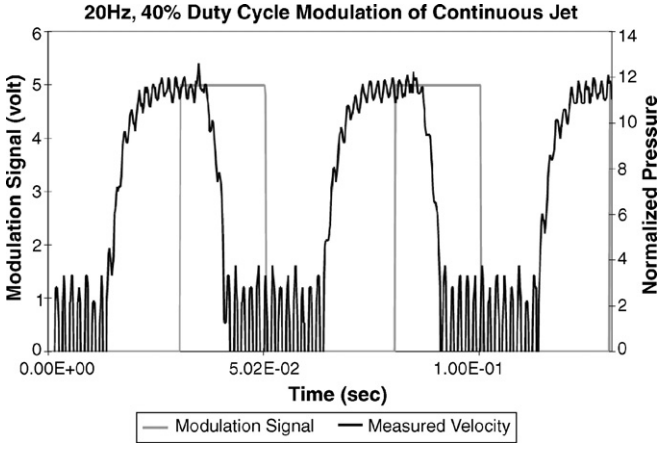

Fig. 13. Measured pressure in a continuous jet modulated with a 20 Hz, 40% duty cycle modulation signal.

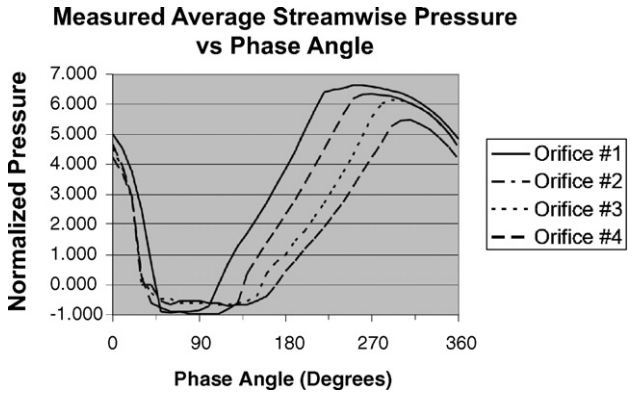

Fig. 14. Variation of jet pressure with phase angle of modulation signal for modulated micromachined synthetic jets.

Moreover, it is apparent that flow sources and flow sinks may be created by selection of modulation phase shifts of 270 or 90°, respectively. This suggests the following application to demonstrate the unique capabilities of modulated synthetic jets.

9. Sample application of phase modulated synthetic jets—lateral air pump

Phase modulation of the flow from two orifices can be used to create a lateral air pump as shown in Fig. 16. From the previous experiments, 90° modulation can be used to turn the right orifice into a flow sink, Fig. 16(a), and 270° modulation can be used to turn the left orifice into a flow source, Fig. 16(b). Simultaneous operation of the flow sink and flow source will result in air being entrained by the right orifice during the first half of the cycle synthetic jet actuation cycle and ejected by the left orifice during the second half of the cycle. For this experiment, flow from the other two orifices was temporarily disabled. Using the pressure tube, the exit pressures of the two orifices were measured. Three phase-locked function generators were used to generate and synchronize the synthetic jet and phase modulation signals. For reference, the pressure of the unmodulated flow was measured (both modulators in their default open position). Both modulation function generators were then activated, simultaneously sending a 270° modulation signal to the

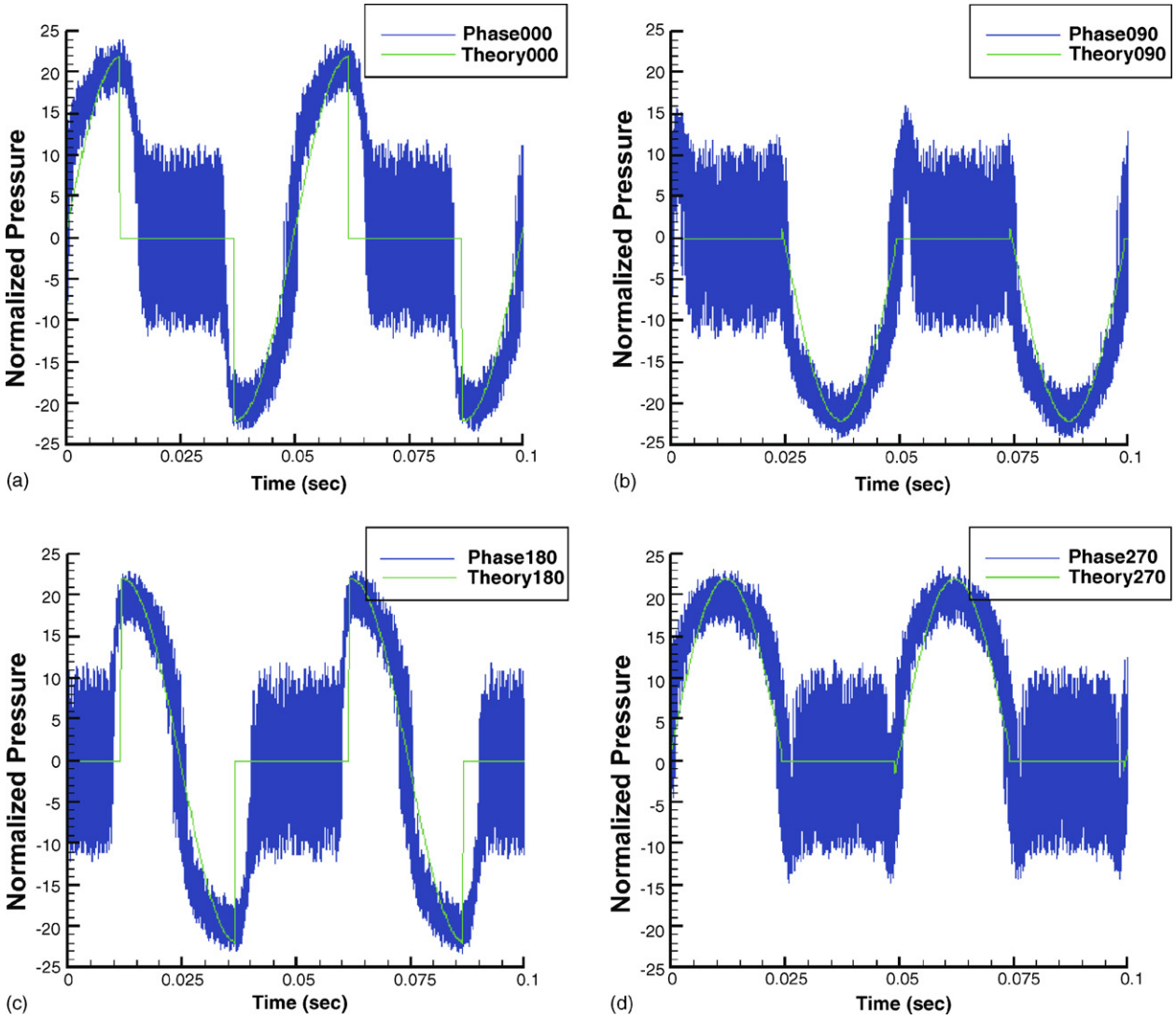

Fig. 15. Comparison of measured of modulated synthetic jet flow. (a) 0° (b) 90° (c) 180° and (d) 270°.

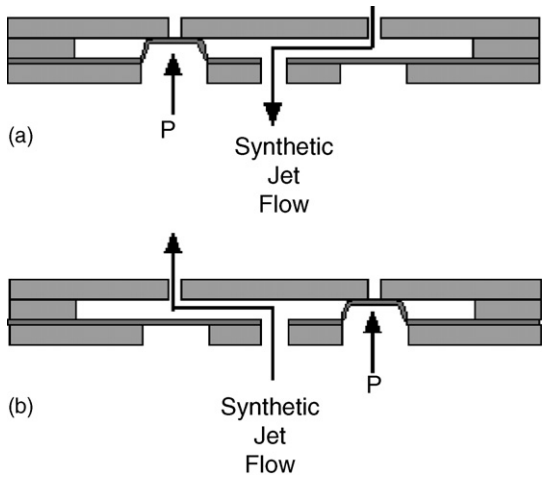

Fig. 16. Pneumatic microjet modulator array operated as an air pump. Synthetic jet intake stroke (a) and discharge stroke (b).

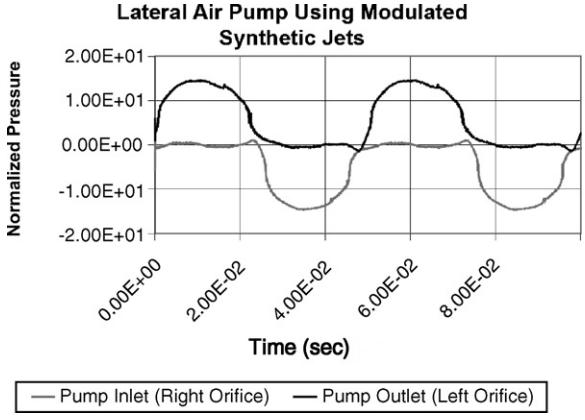

Fig. 17. Measured exit pressure of flow source (270°) and flow sink (90°).

left jet and a 90° modulation signal to the right jet. The measurements of the pressure of the modulated jets are shown in Fig. 17. Note that as predicted the right jet functions as the air pump inlet, as indicated by its negative exit pressure, and the left jet functions as the air pump outlet, as indicated by its positive exit pressure.

10. Conclusions

Pneumatically actuated micromachined synthetic jet modulators have been successfully fabricated, and operation of these devices was verified using both pressure and PIV measurements. In addition to static on-off modulation, dynamic modulation of synthetic jet flows at the jet generation frequency of 20 Hz has also been demonstrated. Continuous variation of the output of individual jets from suction-only operation to exhaust-only operation was achieved by changing the phase of the modulation signal relative to the jet generation signal. A phase formulation of the modulated synthetic jet flow was developed, and agreed reasonably well with pressure measurements at the exit of the modulated synthetic jet array. Most importantly, the use of dynamic synthetic jet flow modulation to create localized regions of non-zero net-mass flux was demonstrated experimentally by using two phase modulated synthetic jets to pump air laterally through a micromachined synthetic jet modulator array. The ability of dynamic synthetic jet flow modulation to create localized flow regions with negative, zero, or positive net mass flux should augment the previously demonstrated capabilities of synthetic jets in jet vectoring and flow control applications by facilitating the generation of more arbitrary two-dimensional flows.

Future work includes the optimization of both synthetic jet performance and microvalve modulator performance, exploration of alternative modulator actuation technologies, and the development improved fabrication and bonding techniques to facilitate higher device densities.

Acknowledgements

The authors would like to thank the sponsors of this research, the Air Force Office of Scientific Research (AFOSR) and the Defense Advanced Research Projects Agency (DARPA), and the staff of the Georgia Tech Microelectronics Research Center for making this research possible.

References

[1] A. Glezer, M.G. Allen, D.J. Coe, B.L. Smith, M.A. Trautman, J.W. Wiltse, Synthetic Jet Actuator and Applications Thereof, United States Patent 5,758,823, Granted June 2, 1998.
[2] B.L. Smith, A. Glezer, The formation and evolution of synthetic jets, Phys. Fluids 10 (1998) 2281–2297.
[3] A. Glezer, M. Amitay, Synthetic jets, Ann. Rev. Fluid Mech. 24 (2002).
[4] M. Amitay, A. Glezer, The role of the actuation frequency in controlled flow reattachment over a stalled airfoil, AIAA J. 40 (2002) 209–216.
[5] B.L. Smith, A. Glezer, Vectoring of adjacent synthetic jets, AIAA J. 43 (2005) 2117–2124.
[6] B.L. Smith, A. Glezer, Vectoring and small-scale motions effected in free shear flows using synthetic jet actuators, AIAA Paper 97-0213, 1997.
[7] M. Amitay, A. Honohan, M. Trautman, A. Glezer, Modification of the aerodynamic characteristics of bluff bodies using fluidic actuators, AIAA Paper 97-2004, 1997.
[8] L. Lagorce, O. Brand, D. Kercher, A. Glezer, M.G. Allen, Micromachined jets for electronic cooling applications, in: IMAPS Proceedings of the 1997 International Symposium on Microelectronics (SPIE vol. 3235), Philadelphia, PA, 1997, pp. 592–597.
[9] T.-K.A. Chou, K. Najafi, M.O. Muller, L.P. Bernal, P.D. Washabaugh, Characterization of micromachined acoustic ejector and its applications, The Fifteenth IEEE International Conference on Micro Electro Mechanical Systems, 2002, pp. 265–267.
[10] K.E. Wu, K.S. Breuer, Dynamics of synthetic jet actuator arrays for flow control, AIAA Paper 2003-4257, Orlando, FL, June 2003.
[11] D.J. Coe, M.G. Allen, M.A. Trautman, A. Glezer, Micromachined jets for manipulation of macro flows, Experimental results presented at the 1994 Solid-State Sensor and Actuator Workshop, Hilton Head, SC, pp. 243–247, June 1994.
[12] D.J. Coe, M.G. Allen, M.A. Trautman, A. Glezer, Addressable Micromachined jet arrays, Eight International Conference on Solid-State Sensors and Actuators and Eurosensors IX, Stockholm, Sweden, pp. 329–332, 1995.
[13] U. Ingard, S. Labate, Acoustic circulation effects and the nonlinear impedance of orifices, J. Acoust. Soc. Am. 22 (1950) 211–219.

Biographies

Dr. David J. Coe received the B.S. degree in computer science from Duke University in Durham, North Carolina, in 1989, and the MSEE and the PhD degrees in electrical engineering from the Georgia Institute of Technology in Atlanta, Georgia, in 1991 and 2002, respectively. His research at Georgia Tech focused on silicon micromachining and the development of micromachined synthetic jet actuators and modulators. He joined the faculty of the University of Alabama in Huntsville as an assistant professor in 2002. His current research interests include micromachined sensors for inertial navigation, chemical and biological sensing, and system health monitoring.

Dr. Mark G. Allen received the BA degree in Chemistry, the BSE degree in chemical engineering and the BSE degree in electrical engineering from the University of Pennsylvania, and the SM and PhD (1989) from the Massachusetts Institute of Technology. In 1989, he joined the faculty of the School of Electrical and Computer Engineering of the Georgia Institute of Technology, where he currently holds the rank of Regents' Professor and the J.M. Pettit Professorship in Microelectronics. His current research interests are in the field of microfabrication and nanofabrication technology, with emphasis on new approaches to fabricate devices with characteristic lengths in the micro- to nanoscale from both silicon and non-silicon materials. Examples include micromagnetics, high temperature sensors, small-scale power generation, biofluidic microvasculatures and implantable microsensors, and the use of microstructures to create nanostructures. Professor Allen was the co-chair of the 1996 IEEE Microelectromechanical Systems Conference.

Christopher S. Rinehart was born in York, Pennsylvania in 1974. He received his BS in engineering mechanics from Johns Hopkins University in 1997. He is currently a PhD candidate at the Georgia Institute of Technology in the School of Mechanical Engineering, with a focus on fluid mechanics. His thesis work involves the study of transitory aerodynamic flow control on bodies of revolution. He also serves in a support capacity for associates in the measurement and characterization of gas generator actuators and the related study of surrogate steady jets.

Dr. Ari Glezer received the Doctor of Philosophy degree from the California Institute of Technology in 1981. In 1992, he joined the Georgia Institute of Technology, where he currently holds the rank of Professor and the Woodruff Chair in Thermal Systems in the School of Mechanical Engineering. His research interests include manipulation and control of turblent shear flows with particular emphasis on aerodynamic lift and drag, mixing processes for combustion applications, thrust vectoring, jet noise, convection-driven flows, and thermal management in electronic packaging. An important aspect of this work has been the development of novel actuator technologies that include piezoelectric and fluidic actuators based on synthetic jets and MEMS-based actuators.